Coercivity mechanism of sintered $Pr_{17}Fe_{75}B_8$ and $Pr_{17}Fe_{53}B_{30}$ permanent magnets

X. C. Kou and H. Kronmüller
Max-Planck-Institut für Metallforschung, Institut für Physik, Heisenbergstrasse I, 70569 Stuttgart, Germany

D. Givord and M. F. Rossignol
Laboratoire Louis Néel, Centre National de la Recherche Scientifique, 166X, 38042 Grenoble-Cedex 9, France
(Received 3 November 1993)

Two coercivity models, a phenomenological model developed by Givord *el al.* and a micromagnetic model developed by Kronmüller *et al.*, have been used to analyze the temperature dependence of the coercive field of sintered $Pr_{17}Fe_{75}B_8$ and $Pr_{17}Fe_{53}B_{30}$ permanent magnets. A general comparison of these two models is made. The micromagnetic model takes into account the misalignment of grains and the anisotropy imperfections at the grain surface. From the analysis based on this model it follows that the coercivity in sintered $Pr_{17}Fe_{75}B_8$ and $Pr_{17}Fe_{53}B_{30}$ permanent magnets is controlled by a nucleation mechanism occurring preferentially in the grain surface where the magnetic anisotropy is reduced and the local demagnetizing field is the highest. A simple proportional relationship between the micromagnetic parameters and N_{eff} is found. In addition, the effect of magnetic coupling among grains can be estimated with this model. The phenomenological model takes into account the geometrical effect of nucleated domains, the effect of the disturbance of domain-wall energy, and the thermal activation. From the analysis based on this model, it follows that the expansion of reversed domains takes place preferentially in regions where the domain-wall energy is reduced and where a spikelike reversed domain is energetically favorable. It is demonstrated in the present investigation that the phenomenological model corresponds approximately to the micromagnetic model when the nucleation process dominates the magnetization reversal process and the magnetic coupling between grains is weak.

I. INTRODUCTION

Coercivity is an essential magnetic property, which characterizes the hardness of the magnetic materials. The coercivity is measured by the value of the coercive field H_C, the inverse field necessary to obtain zero macroscopic magnetization from the saturation. The origin of coercivity in rare-earth permanent magnets is the uniaxial magnetocrystalline anisotropy. It must be noted that the coercivity is not an intrinsic magnetic property, which means that the value of the coercive field H_C as well as the magnetization reversal process depends not only on the chemical composition, the temperature and the magnetic anisotropy, but also strongly on the microstructure of the materials. In order to understand the coercivity mechanism in rare-earth intermetallic compounds, different types of rare-earth permanent magnets have been studied, $SmCo_5$ type,[1] Sm_2Co_{17} type,[2] and NdFeB type.[3–16] In a first approximation it was assumed that the magnetization is reversed uniformly and coherently under the action of the applied inverse field.[17] In this case the value of the coercive field corresponds to the value of the nucleation field, $2K_1/M_s$ (K_1 is the second-order magnetocrystalline anisotropy constant and M_s is the spontaneous magnetization of the hard magnetic phase) of materials. However, this assumption fails in all practical permanent magnetic materials found up to now.[4,5,7–9] The reason is that practical magnetic materials are inhomogeneous and consist of domains (in most cases multidomains), which offer an energy-favorable region for magnetization reversal. The magnetization reversal process actually begins with a nucleation of an energy-favorable reverse domain and develops with a spontaneous propagation of the nucleated (reversed) domain throughout the grains. According to this argument, two basic mechanisms, nucleation or pinning controlled, can be proposed for real permanent magnets. Accordingly, the nucleation of a reversed domain is necessary for both mechanisms. It is well accepted that the coercivity mechanism of the sintered $SmCo_5$ and NdFeB-type magnets is controlled by the nucleation process, whereas the pinning process plays a leading role in determining the coercivity of Sm_2Co_{17}-type multiphase magnets.[18]

Compared to numerous studies performed on Nd-Fe-B permanent magnets (see review by Herbst[19] and the papers cited therein), only a few studies have been reported on Pr-Fe-B magnets.[15,20–23] A spin-reorientation transition occurs in Nd-Fe-B permanent magnets at low temperature, which makes the analysis of the temperature dependence of the coercive field below 200 K rather complicated.[4,24] In the present investigation, Pr-Fe-B permanent magnets were chosen in order to avoid this difficulty. In addition, the rather large value of K_1 ($>4K_2$), the second-order anisotropy constant, in the whole magnetically ordered temperature range of $Pr_2Fe_{14}B$ (the hard magnetic phase in Pr-Fe-B magnets) makes it a better candidate material for a test of theoretical prediction.

Presently, two models have been proposed for describ-

ing the coercivity of rare-earth permanent magnets. One is a phenomenological model based on energetically arguments and is developed by Givord and co-workers,[10–14] and the other is a micromagnetic model based on the eigenvalues of the micromagnetic equation and is developed by Kronmüller and co-workers.[3,4,25] Both have been applied successfully for the Nd-Fe-B magnets.[4,10,14] In the present investigation, the analysis based on both of these two models is extended to Pr-Fe-B magnets and an effort is made to compare these two models.

The present paper is organized as follows: Section II gives the intrinsic magnetic properties of Pr-Fe-B magnets, while experimental details and the experimental results have been described in Sec. III; Secs. IV and V show in detail the analysis based on the two coercivity models; in Sec. VI, the two coercivity models are compared based on the analysis of Secs. IV and V; and finally, in Sec. VI a summary is given.

II. INTRINSIC MAGNETIC PROPERTIES OF Pr-Fe-B PERMANENT MAGNETS

Both, $Pr_{17}Fe_{75}B_8$ and $Pr_{17}Fe_{53}B_{30}$, magnets have the same magnetic phase $Pr_2Fe_{14}B$ as the matrix phase. Therefore, the intrinsic magnetic properties, i.e., anisotropy constants, spontaneous magnetization, etc., are the same as in $Pr_2Fe_{14}B$ for both magnets. The anisotropy constants K_1 and K_2 of $Pr_2Fe_{14}B$ have been determined up to 500 K from crystalline electric-field (CEF) calculations (see Fig. 1). The CEF parameters have been obtained by fitting the magnetization curves measured on the $Pr_2Fe_{14}B$ single crystal along different crystallographic directions and at various temperatures. The spontaneous magnetization M_s and its temperature dependencies were also determined by these measurements. Particular emphasis was given to the magnetic phase transitions, the first-order magnetization process (FOMP) and the spin reorientation, that strongly limits CEF parameters.[26,27] The details of the CEF calculation can be found in the literature.[28–30] The exchange constant A was estimated from the value of the Curie temperature. The temperature dependence of $A(T)$ is obtained by assuming that

$$A(T)=\left[\frac{M_s(T,Y_2Fe_{14}B)}{M_s(0,Y_2Fe_{14}B)}\right]^2 A(0) .$$

The data for $M_s(T,Y_2Fe_{14}B)$ have been taken from literature.[31] For the 180° domains as observed in Pr-Fe-B magnets, the domain-wall energy γ is determined by[32]

$$\gamma(T)=\sqrt{A(T)}\int_0^{\pi}\sqrt{E(\theta,T)}d\theta ,$$

and the domain-wall width δ_B is determined by[32]

$$\delta_B(T)=\sqrt{A(T)}\int_0^{\pi}\frac{1}{\sqrt{E(\theta,T)}}d\theta ,$$

where $E(\theta)$ is anisotropy energy given by

$$E(\theta,T)=K_1\sin^2\theta+K_2\sin^4\theta+\cdots ,$$

and θ is the angle between the c axis and the magnetization, whereas K_1 and K_2, etc., are the anisotropy constants. Details of the calculation have been published previously.[32]

III. EXPERIMENTAL DETAILS AND RESULTS

The sintered permanent magnets of compositions $Pr_{17}Fe_{75}B_8$ and $Pr_{17}Fe_{53}B_{30}$ were provided by S. Hirosawa of the Sumitomo company, Japan. $Pr_{17}Fe_{75}B_8$ (three-phase magnet) contains more than 84% (volume) of the matrix phase, known as the $Pr_2Fe_{14}B$ phase. The other phases are Pr-rich ($Pr_{1-x}Fe_x$) and B-rich phases ($PrFeB_{4\pm\varepsilon}$). In the case of $Pr_{17}Fe_{53}B_{30}$ (two-phase magnet), only 33% (volume) corresponds to the $Pr_2Fe_{14}B$ phase. The rest is the B-rich $PrFeB_{4\pm\varepsilon}$ phase.[20–23] It is interesting to note that the single-phase $Pr_2Fe_{14}B$ magnets show a very small coercive field, suggesting the importance of the grain bounding phases in establishing the coercivity of an anisotropy intermetallic compound. The temperature dependence of the coercive field H_C of $Pr_{17}Fe_{75}B_8$ and $Pr_{17}Fe_{53}B_{30}$ magnets, as shown in Fig. 2, has been measured from 25 to 500 K in a vibrating sample magnetometer (VSM) equipped with a superconducting magnet. The $Pr_{17}Fe_{53}B_{30}$ magnet generally shows larger values of the coercive field H_C. The temperature dependence of the magnetic viscosity coefficient S_V ($=S/\chi_{irr}$, where $S=dM/d\ln T$ and χ_{irr} is the irreversible susceptibility) of these two magnets has been determined by using the VSM in the same temperature range (see Fig. 3).

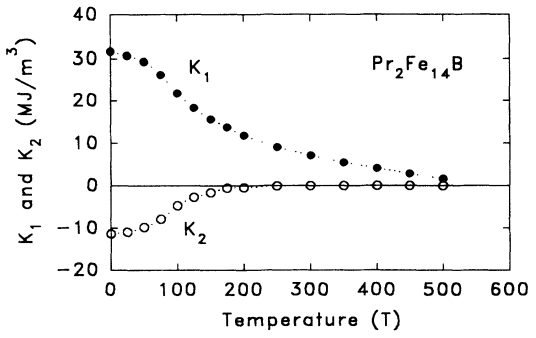

FIG. 1. Temperature dependence of the anisotropy constants K_1 and K_2 of $Pr_2Fe_{14}B$.

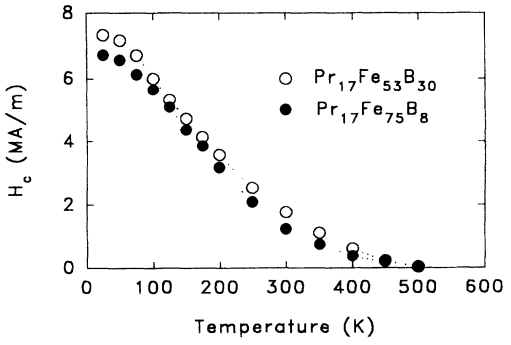

FIG. 2. Temperature dependence of the coercive field H_C of $Pr_{17}Fe_{75}B_8$ and $Pr_{17}Fe_{53}B_{30}$.

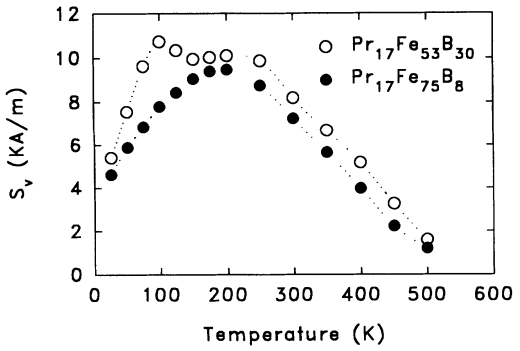

FIG. 3. Temperature dependence of magnetic viscosity coefficient S_v for $Pr_{17}Fe_{75}B_8$ and $Pr_{17}Fe_{53}B_{30}$.

IV. ANALYSIS OF THE TEMPERATURE DEPENDENCE OF THE COERCIVE FIELD OF $Pr_{17}Fe_{75}B_8$ AND $Pr_{17}Fe_{53}B_{30}$ BASED ON THE PHENOMENOLOGICAL MODEL

According to the phenomenological model,[10–14] the coercive field H_C can be expressed as

$$H_C=\alpha\frac{\gamma}{\mu_0 M_s v_a^{1/3}}-N_{\text{eff}}M_s-25S_v\ , \tag{1}$$

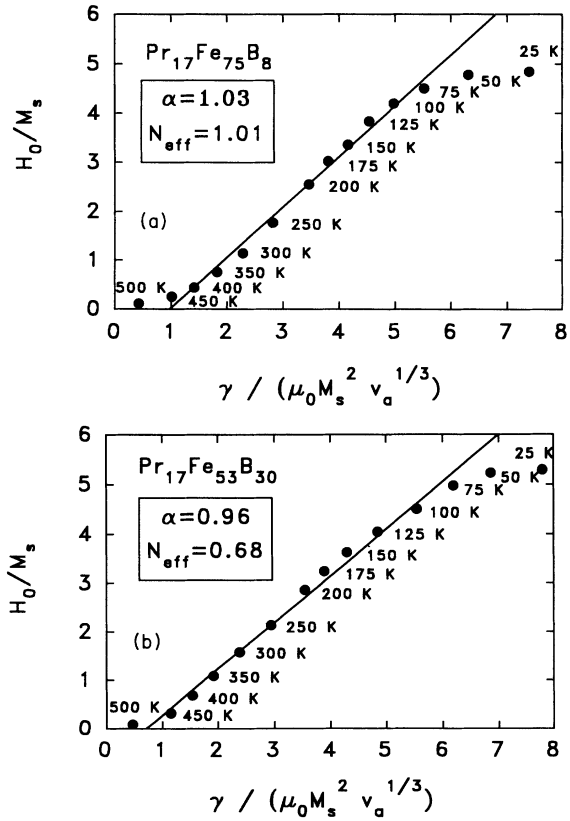

FIG. 4. (a) The plot of H_0/M_s vs $\gamma/\mu_0 M_s^2 v_a^{1/3}$ for $Pr_{17}Fe_{75}B_8$ for testing the phenomenological model. (b) The plot of H_0/M_s vs $\gamma/\mu_0 M_s^2 v_a^{1/3}$ for $Pr_{17}Fe_{53}B_{30}$ for testing the phenomenological model.

where γ, M_s, and v_a are the domain-wall energy, the spontaneous magnetization of $Pr_2Fe_{14}B$ and the thermal activation volume, respectively. The activation volume is given by $v_a=kT/\mu_0 M_s S_v$. All these parameters can be determined experimentally. α is a complex coefficient and N_{eff} is an effective demagnetizing factor. It is worthwhile to note that within the framework of this model neither α nor N_{eff} are temperature dependent. The physical meaning of α remains to be clarified. N_{eff} is a macroparameter, which describes the average demagnetizing factor over all grains in a magnet.

In this expression, the first term on the right is the energy barrier at the origin of the coercivity. The second term is the demagnetizing field, which assists in nucleating a reverse domain, and the third term is due to the thermal activation. However, the actual value of the third term is much smaller than that of the other two terms, suggesting that the nucleation of a reversed domain is actually not due to thermal activation.

Figures 4(a) and 4(b) show the plot of H_0/M_s versus $\gamma/(\mu_0 M_s^2 v_a^{1/3})$ at various temperatures from 25 up to 500 K for $Pr_{17}Fe_{75}B_8$ and $Pr_{17}Fe_{53}B_{30}$, where $H_0=H_C+25S_v$. It is found that a linear relationship can only be found in the temperature range between 75 and 450 K. By using a least-squares-fitting program, the coefficients α and N_{eff} were determined and shown in Figs. 4(a) and 4(b). It is evident that the fitted values of α are close to 1 and remain constant, whereas the values of N_{eff} varies from one magnet to another, reflecting its dependence on microstructure, i.e., shape and size of grains and the environment surrounding the grains.[3,9] The $Pr_{17}Fe_{53}B_{30}$ magnet has smaller N_{eff} than the $Pr_{17}Fe_{75}B_8$ magnet. This might be the reason for the higher coercive field of the $Pr_{17}Fe_{53}B_{30}$ magnet. From this analysis it follows that it is not possible to draw a conclusion concerning the description of the real magnetization reversal process.

V. ANALYSIS OF TEMPERATURE DEPENDENCE OF THE COERCIVE FIELD OF $Pr_{17}Fe_{75}B_8$ AND $Pr_{17}Fe_{53}B_{30}$ BASED ON THE MICROMAGNETIC MODEL

According to the micromagnetic model,[3–9,25] the coercive field H_C of an uniaxial anisotropy magnet can be generally expressed as ($K_1>4K_2$)

$$H_C=\frac{2K_1}{\mu_0 M_s}\alpha_K\alpha_\varphi^{\text{eff}}-N_{\text{eff}}M_s\ , \tag{2}$$

where K_1, M_s, and N_{eff} are the second-order anisotropy constant, the spontaneous magnetization determined for $Pr_2Fe_{14}B$ and the local effective demagnetization factor, respectively. α_K and N_{eff} are the micromagnetic as well as the microstructural coefficients. The former describes the anisotropy inhomogeneity range where a reversed domain nucleates, whereas the latter describes the misalignment of grains and depends sensitively on the values of the high-order anisotropy constants. Different to the phenomenological model, both α_K and $\alpha_\varphi^{\text{eff}}$ are temperature dependent.

In this expression, the first term on the right-hand side of Eq. (2) is the effective nucleation field and is determined only by the intrinsic parameters of the hard magnetic phase $Pr_2Fe_{14}B$. N_{eff} is a microparameter, which corresponds to the highest demagnetizing factor of the grains with the misaligned angle described by $\alpha_\varphi^{\text{eff}}$. The physical meaning of $\alpha_\varphi^{\text{eff}}$ and N_{eff} is evident within the framework of this model. $\alpha_\varphi^{\text{eff}}$ is correlated to these grains, which reverse magnetization preferentially. N_{eff} gives the exact place, on the surface of these preferentially reversed grains, where the reversed domain is preferentially nucleated.

It has been shown theoretically that these two coercivity mechanisms, i.e., the pinning and the nucleation controlled, results in rather different microstructural coefficients. In the case of the nucleation controlled magnets, the micromagnetic parameters $\alpha_\varphi^{\text{eff}}$ and α_K^{nucl} of an isolated grain can be calculated by[3-9]

$$\alpha_\varphi^{\text{eff}}=\frac{1}{\cos\varphi}\frac{1}{(1+\tan^{2/3}\varphi)^{3/2}}\left[1+\frac{2K_2}{K_1}\frac{\tan^{2/3}\varphi}{1+\tan^{2/3}\varphi}\right], \tag{3}$$

where φ is the angle between the applied field and the negative c axis, and

$$\alpha_K^{\text{nucl}}=1-\frac{1}{4\pi^2}\frac{\delta_B^2}{r_0^2}\left[-1+\left[1+\frac{4\Delta K r_0^2}{A}\right]^{1/2}\right]^2, \tag{4}$$

where δ_B, ΔK, A, and r_0 are the domain-wall width, a reduction of the anisotropy constant K_1 by ΔK, the exchange constant and the half width of the planar perturbed inhomogeneous region of width $2r_0$, respectively. The theoretical calculation leads to the condition for nucleation that $\alpha_K>0.3$, where the values of $\alpha_\varphi^{\text{eff}}$ can be calculated from Eq. (3) taking into account the magnetic coupling between the magnetic grains.

In the case of pinning controlled magnets,

$$\alpha_\varphi^{\text{eff}}=\alpha_\varphi^{\text{pin}}=\frac{1}{\cos\varphi},$$

$$\alpha_K=\alpha_K^{\text{pin}},$$

and the values of α_K^{pin} depend strongly on the type of the pinning centers, leading to the condition that $\alpha_\varphi^{\text{eff}}=1$ and $\alpha_K^{\text{max}}=0.3$.

Therefore, from the comparison of the coefficients obtained from the calculation based on the micromagnetic theory and the coefficients obtained by fitting the experimental data, the actual mechanism, which controls the coercivity of the materials can be determined. Since the analysis based on this model gives a clear distinction of the magnetization reversal process, the analysis has to be divided into two principal steps, i.e., the pinning mechanism and the nucleation mechanism.

A. Test of the pinning mechanism

According to the micromagnetic theory,[25,33,34] if the domain wall is pinned by thin planar inhomogeneities ($r_0<\delta_B$), H_C can be expressed by

$$H_C=\frac{1}{3\sqrt{3}}\frac{2K_1}{\mu_0 M_s}\frac{\pi}{\delta_B}r_0-N_{\text{eff}}M_s, \tag{5}$$

and comparison to Eq. (2) gives $\alpha_\varphi^{\text{eff}}=1$ and $\alpha_K^{\text{pin}}=\pi r_0/3\sqrt{3}\delta_B$. If the domain wall is pinned by extended planar inhomogeneities ($r_0>\delta_B$), H_C is expressed by[3]

$$H_C=\frac{2K_1}{\mu_0 M_s}\frac{2\delta_B}{3\pi}\frac{1}{r_0}-N_{\text{eff}}M_s. \tag{6}$$

In this case, comparison to Eq. (2) gives $\alpha_\varphi^{\text{eff}}=1$ and $\alpha_K^{\text{pin}}=2\delta_B/3\pi r_0$. Here r_0 is the average value of the half width of the inhomogeneities and δ_B is the domain-wall width.

1. *Thin planar inhomogeneities* ($r_0<\delta_B$)

Figures 5(a) and 5(b) show the plots of H_C/M_s versus $2\pi K_1/3\sqrt{3}\delta_B\mu_0 M_s^2$ for $Pr_{17}Fe_{75}B_8$ and $Pr_{17}Fe_{53}B_{30}$, respectively. The purpose for doing this is to test if the coercivity is controlled by a pinning center of thin inhomogeneities. It follows from these figures that a linear relation exists only in a very limited temperature range,

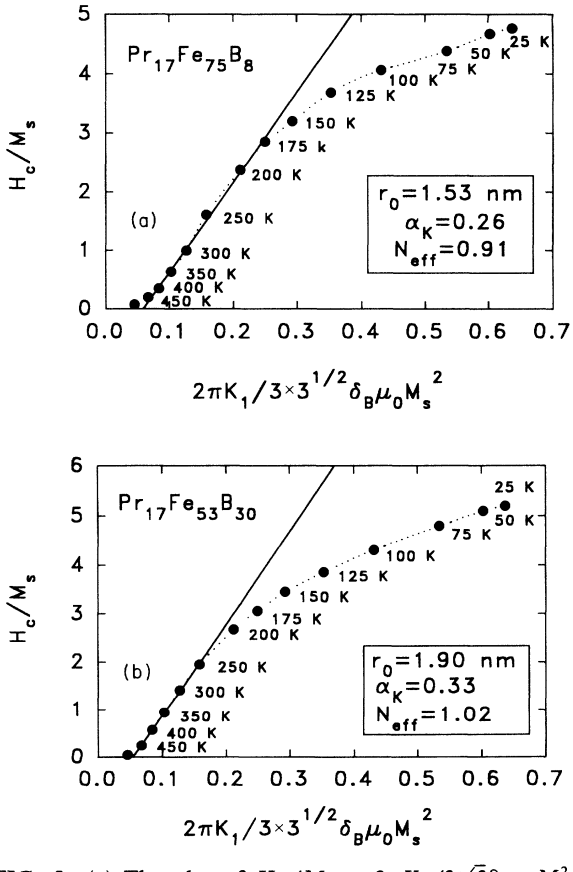

FIG. 5. (a) The plot of H_C/M_s vs $2\pi K_1/3\sqrt{3}\delta_B\mu_0 M_s^2$ for $Pr_{17}Fe_{75}B_8$ for testing the pinning model where the pinning centers are thin planar inhomogeneities. (b) The plot of H_C/M_s vs $2\pi K_1/3\sqrt{3}\delta_B\mu_0 M_s^2$ for $Pr_{17}Fe_{53}B_{30}$ for testing the pinning model where the pinning centers are thin planar inhomogeneities.

e.g., from 250 to 450 K for $Pr_{17}Fe_{53}B_{30}$ and from 175 to 400 K for $Pr_{17}Fe_{75}B_8$. The values of r_0 and N_{eff} have been estimated by fitting this linear relationship. We obtained $r_0=1.90$ nm, $N_{\text{eff}}=1.02$ for $Pr_{17}Fe_{53}B_{30}$ and $r_0=1.53$ nm, $N_{\text{eff}}=0.91$ for $Pr_{17}Fe_{75}B_8$. The values of α_K^{pin} are temperature dependent and the data of α_K^{pin} at 300 K have been calculated [see Figs. 5(a) and 5(b)]. For $Pr_{17}Fe_{53}B_{30}$, the fitted values of r_0 and N_{eff} are reasonable. However, the calculated values of α_K^{pin} are always larger than 0.3, the maximum achievable value of the pinning mechanism, over the whole fitted temperature. This suggests that thin inhomogeneities play no role in determining coercivity in $Pr_{17}Fe_{53}B_{30}$ magnets. For $Pr_{17}Fe_{75}B_8$, the fitted values of r_0 and N_{eff} are also reasonable. The calculated values of α_K^{pin} are smaller than 0.3 only in the temperature range from 250 to 400 K. This indicates that thin inhomogeneities may play some role in determining the coercivity of $Pr_{17}Fe_{75}B_8$. However, this is the case only in a rather limited temperature range. From the value of $2r_0=3.06$ nm it follows that the actual inhomogeneities here are limited to point defects or dislocations.

2. *Extended planar inhomogeneities* ($r_0 > \delta_B$)

Figures 6(a) and 6(b) show the plots of H_C/M_s versus $4\delta_B K_1/3\pi\mu_0 M_s^2$ for $Pr_{17}Fe_{75}B_8$ and $Pr_{17}Fe_{53}B_{30}$, respectively. The purpose for doing this is to test whether the coercivity is controlled by extended planar inhomogeneities. It follows from these figures that a linear relation exists only in a very limited temperature range, e.g., from 200 to 400 K for $Pr_{17}Fe_{53}B_{30}$ and from 175 to 450 K for $Pr_{17}Fe_{75}B_8$. The values of r_0 and N_{eff} can be estimated by fitting this linear relationship. We obtained $r_0=0.90$ nm, $N_{\text{eff}}=4.66$ for $Pr_{17}Fe_{53}B_{30}$ and $r_0=0.97$ nm, $N_{\text{eff}}=4.55$ for $Pr_{17}Fe_{75}B_8$. These values obtained for r_0 are in contradiction to the assumption $r_0 > \delta_B$. The values of N_{eff} are much too large to have a physical meaning. Additionally, the values of α_K^{pin} at 300 K calculated are 0.77 for $Pr_{17}Fe_{75}B_8$ and 0.83 for $Pr_{17}Fe_{53}B_{30}$, respectively, which are again much too large to be in agreement with a pinning mechanism where $\alpha_K^{\max}=0.3$. Therefore, it can be concluded that the extended inhomogeneities play no role in determining the coercivity in Pr-Fe-B magnets. From the above analysis, it is concluded that the pinning mechanism is not the leading mechanism in determining the coercivity of the sintered Pr-Fe-B permanent magnets.

B. Test of the nucleation mechanism

The analysis based on the micromagnetic model for the nucleation mechanism will be performed in the following steps.

(a) H_C/M_s was plotted as a function of $2K_1/\mu_0 M_s^2$ in order to test if magnetization reverses uniformly. Figures 7(a) and 7(b) show the plots for $Pr_{17}Fe_{75}B_8$ and $Pr_{17}Fe_{53}B_8$, respectively. It can be seen that a linear relationship exists within the temperature range from 200 to 450 K for both investigated magnets. If the magnetization would rotate uniformly and coherently in the Pr-Fe-B magnets, the slope of this line should be 1. In fact, the fitted result shows that the slope of the line is around 0.4 [see Figs. 7(a) and 7(b)]. Therefore, it is concluded that the actual magnetization reversal process in Pr-Fe-B magnets occurs nonuniformly. This suggests that there are no collective processes involved in the magnetization reversal process.

(b) According to Eq. (3), $\alpha_\varphi^{\text{nucl}}$ can be computed at various temperatures taking into account the temperature dependence of K_1 and K_2. For a quantitative analysis of the coercivity, we have to take into account that in general a probability distribution $p(\varphi)$ of misaligned grains exists. Therefore, the effective $\alpha_\varphi^{\text{eff}}$ values representative for H_C have to be determined by an appropriate averaging. The type of averaging depends strictly on the magnetic coupling between neighboring grains. As proposed previously,[4] two extreme cases are considered.

1. *Strongly magnetically coupled grains*

In this case,

$$\alpha_\varphi^{\text{eff}}=\alpha_\varphi^{\min},$$

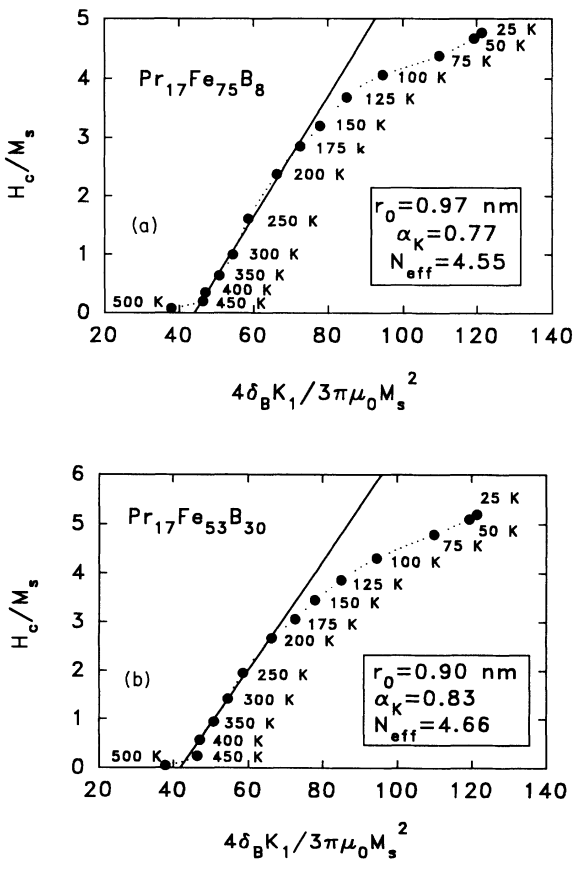

FIG. 6. (a) The plot of H_C/M_s vs $4\delta_B K_1/3\pi\mu_0 M_s^2$ for $Pr_{17}Fe_{75}B_8$ for testing the pinning model where the pinning centers are extended planar inhomogeneities. (b) The plot of H_C/M_s vs $4\delta_B K_1/3\pi\mu_0 M_s^2$ for $Pr_{17}Fe_{53}B_{30}$ for testing the pinning model where the pinning centers are extended planar inhomogeneities.

where $\alpha_\varphi^{\min}$ is the minimum of $\alpha_\varphi^{\text{nucl}}$ of Eq. (3). If all grains are strongly magnetically coupled a reversion of a misaligned grain induces also the reversion of neighboring grains. The bulk coercive field depends, therefore, only on these grains, which have the minimum nucleation field. According to this assumption, Eq. (2) is transformed into[5]

$$H_C=\frac{2K_1}{\mu_0 M_s}\alpha_K\alpha_\varphi^{\min}-N_{\text{eff}}M_s \ .$$

In this case, the coercive field H_C, a macromagnetic property (extrinsic), is determined only by the minimum nucleation field, a micromagnetic property (intrinsic) of these grains, which make an angle φ_0 with the direction of the applied field. This approximation is justified by recent model calculation by Schrefl.[38] The value of φ_0 corresponds to the angle, where $\alpha_\varphi^{\text{nucl}}$ has its minimum value. Since wherever the external field is applied, there are always grains, which make an angle φ_0 with the applied field. Therefore, the coercive field H_C of an imperfectly aligned bulk magnet should be angular independent in the case that this assumption is valid. In fact, the angular dependence of the coercive field has been detected experimentally,[11,21] suggesting that in this case the value of

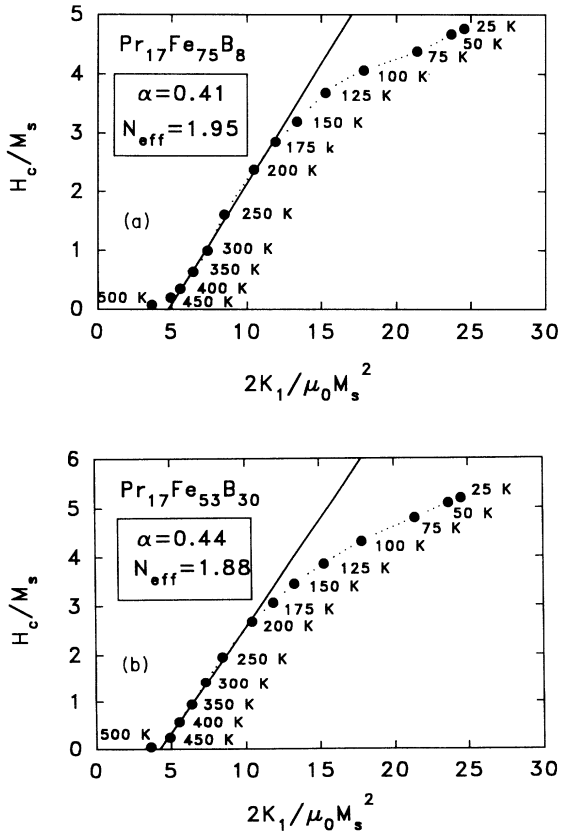

FIG. 7. (a) The plot of H_C/M_s vs $2K_1/\mu_0 M_s^2$ for $Pr_{17}Fe_{75}B_8$ for testing the nucleation model under the assumption that magnetization reverses coherently. (b) The plot of H_C/M_s vs $2K_1/\mu_0 M_s^2$ for $Pr_{17}Fe_{53}B_{30}$ for testing the nucleation model under the assumption that magnetization reverses coherently.

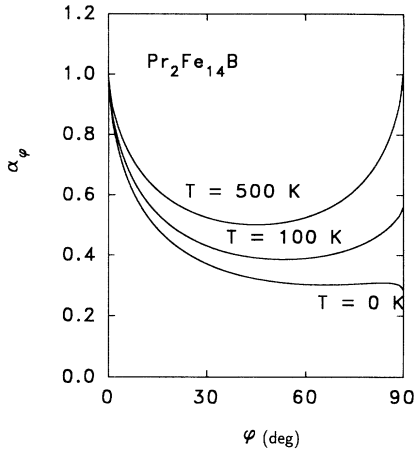

FIG. 8. Angular dependence of $\alpha_\varphi^{\text{nucl}}$ calculated for $Pr_2Fe_{14}B$ at $T=0$, 100, and 500 K.

$\alpha_\varphi^{\text{eff}}$ ($=\alpha_\varphi^{\min}$) is underestimated. Therefore, the $\alpha_\varphi^{\min}$ is the lowest limit for $\alpha_\varphi^{\text{eff}}$.

For a given temperature, the angular dependence of $\alpha_\varphi^{\text{eff}}$ of Pr-Fe-B can be computed with Eq. (3) for various angles from 0° to 90°. Figure 8 gives the computed results at 100, 300, and 500 K. The value of $\alpha_\varphi^{\min}$ can be obtained accordingly (see Fig. 9). It is of interest to note that the angle (φ_0), where $\alpha_\varphi^{\text{eff}}$ is minimum is far from 45°, particularly at low temperature, where the values of the high-order anisotropy constant K_2 are large, e.g., $\varphi_0=66°$, 62°, and 53° at 0, 50, and 100 K.

2. *Magnetically isolated grains*

In this case,

$$\alpha_\varphi^{\text{eff}}=\alpha_\varphi^{\text{int}}=\int P(\varphi)\alpha_\varphi^{\text{nucl}}d\varphi \ , \tag{7}$$

where $P(\varphi)$ is an appropriate distribution function, which describes the probability of the misaligned grains and follows the relation

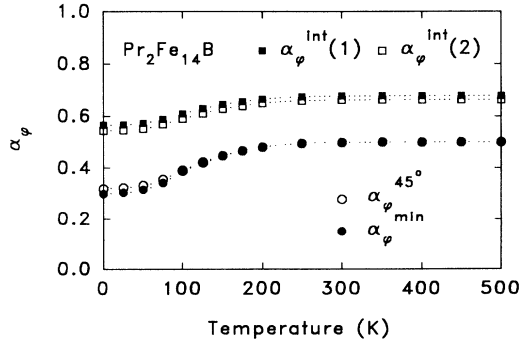

FIG. 9. Temperature dependence of $\alpha_\varphi^{\min}$, $\alpha_\varphi^{\text{int}}$, and $\alpha_\varphi^{45°}$ calculated for Pr-Fe-B magnets. $\alpha_\varphi^{\min}$ is the minimum of $\alpha_\varphi^{\text{eff}}$ and $\alpha_\varphi^{45°}$ is the value of $\alpha_\varphi^{\text{eff}}$ in the case of $\theta=45°$. $\alpha_\varphi^{\text{int}}(1)$ has been calculated for the distribution function $p(\theta)=0.85N(0,18.7)+0.15N(0,36)$. $\alpha_\varphi^{\text{int}}(2)$ has been calculated for the distribution function of $P(\theta)=0.9N(0,17)+0.1N(0,28)$.

$$\int_{-\pi/2}^{\pi/2} P(\varphi)d\varphi=1 \ . \tag{8}$$

The physical meaning of this assumption is that the magnetically isolated grains reverse their magnetization individually without influencing the neighboring grains and thus not influencing $P(\varphi)$. The magnetization reversal process is complete only when the last grain is individually reversed. Therefore, it is evident that the values of $\alpha_\varphi^{\text{eff}}$ are overestimated. $\alpha_\varphi^{\text{int}}$ represents an upper limit of $\alpha_\varphi^{\text{eff}}$. In this case, N_{eff} becomes a macroparameter and therefore, is comparable, principally, to the N_{eff} of the phenomenological model.

According to a study performed on sintered Nd-Fe-B magnets,[35] the misalignment of grains could be described by the Gauss-normal distribution function $N(\mu,\sigma)$, where

$$N(\mu,\sigma)=c\frac{1}{\sigma\sqrt{2\pi}}\exp\left[-\frac{(\varphi-\mu)^2}{2\sigma^2}\right], \quad -\pi/2<\varphi<-\pi/2 , \quad \sigma>0 , \quad -\pi/2<\mu<\pi/2 , \tag{9}$$

and the constant c is determined by

$$\int_{\pi/2}^{\pi/2} N(\mu,\sigma)d\varphi=1 \ . \tag{10}$$

From the x-ray diffraction analysis,[35] $P(\varphi)$ is determined to be

$$P(\varphi)=0.85N(0,18.7)+0.15N(0,36) , \tag{11}$$

as shown in Fig. 10. From this distribution function, it is deduced that more than 99% of the grains have an angle less than 55° away from the alignment direction. The temperature dependence of $\alpha_\varphi^{\text{int}}$, so obtained, is shown in Fig. 9.

Figures 11(a) and 11(b) show the plot of H_C/M_s versus $2\alpha_\varphi^{\min}K_1/\mu_0M_s^2$ for $Pr_{17}Fe_{75}B_8$ and $Pr_{17}Fe_{53}B_{30}$, respectively. The purpose for doing this is to test whether the coercivity of $Pr_{17}Fe_{75}B_8$ and $Pr_{17}Fe_{53}B_{30}$ is controlled by the nucleation mechanism in the case that $\alpha_\varphi^{\text{eff}}=\alpha_\varphi^{\min}$, i.e., strongly magnetically coupled grains. It is evident that a nearly perfect linear relationship exists over the whole investigated temperature range from 25 up to 450 K. By using a least-squares-fitting program, the micromagnetic parameters α_K and N_{eff} were determined [see Figs. 11(a) and 11(b)]. Compared to the macroparameter N_{eff} deduced from the phenomenological model [Figs. 4(a) and 4(b)], the microparameter N_{eff} determined in this case is much larger. This large difference in N_{eff} arises from their different physical meanings. The microparameter N_{eff} of the micromagnetic model describes the local effective demagnetizing field ($-N_{\text{eff}}M_s$) and corresponds to the highest demagnetizing field, giving the region where the reversed domain is preferentially nucleated. However, the macroparameter N_{eff} of the phenomenological model describes the average demagnetizing field ($-N_{\text{eff}}M_S$) and represents the average demagnetizing field over all grains. The detail of this effect will be discussed in Sec. VI A.

Figures 12(a) and 12(b) show the plot of H_C/M_s versus $2\alpha_\varphi^{\text{int}}K_1/\mu_0M_s^2$ for $Pr_{17}Fe_{75}B_8$ and $Pr_{17}Fe_{53}B_{30}$, respectively, in order to test whether the coercivity of $Pr_{17}Fe_{75}B_8$ and $Pr_{17}Fe_{53}B_{30}$ is controlled by the nucleation mechanism in the case that $\alpha_\varphi^{\text{eff}}=\alpha_\varphi^{\text{int}}$, i.e., magnetically isolated grains. Compared with Figs. 11(a) and 11(b), the linear

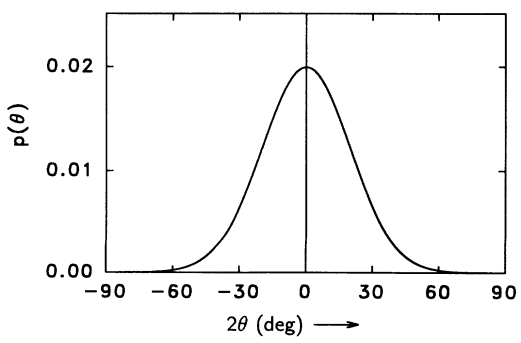

FIG. 10. The angle (reference to the alignment direction) distribution function, $p(\theta)=0.85N(0,18.7)+0.15N(0,36)$, of the sintered Pr-Fe-B magnets.

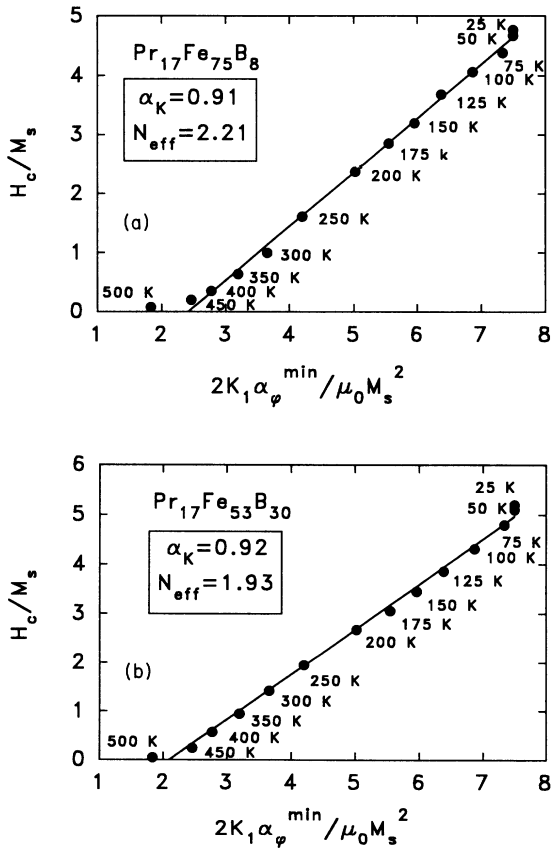

FIG. 11. (a) The plot of H_C/M_s vs $2\alpha_\varphi^{\min}K_1/\mu_0M_s^2$ for $Pr_{17}Fe_{75}B_8$ for testing the nucleation model under the assumption that grains are strongly magnetically coupled. (b) The plot of H_C/M_s vs $2\alpha_\varphi^{\min}K_1/\mu_0M_s^2$ for $Pr_{17}Fe_{53}B_{30}$ for testing the nucleation model under the assumption that grains are strongly magnetically coupled.

relationship of Figs. 12(a) and 12(b) is far from satisfactory. By using a least-squares-fitting program, the micromagnetic parameter α_K and the macroparameter N_{eff} were determined [see Figs. 12(a) and 12(b)]. As is mentioned just above, the N_{eff} determined in the present case becomes a macroparameter. As can be seen from Figs. 4(a) and 4(b), the macroparameter N_{eff} deduced in the present case is comparable to the macroparameter N_{eff} determined from the analysis of the phenomenological model. Comparison of the analysis based on both models, the phenomenological model and the micromagnetic model, gives an evident common conclusion, i.e., the $Pr_{17}Fe_{53}B_{30}$ magnet has smaller N_{eff} than $Pr_{17}Fe_{75}B_8$. This is the reason why the $Pr_{17}Fe_{53}B_{30}$ magnet has the higher coercive field.

The above analysis has been made on the assumption that α_K is temperature independent. From Eq. (4) it follows that the temperature dependency of α_K depends strongly on the value of ΔK, the reduction of K_1. A larger value of ΔK leads to a stronger temperature dependence of α_K. The actual value of ΔK depends predominantly on the magnetic inhomogeneities at the grain surfaces. In the case of $\alpha_\varphi^{\text{eff}}=\alpha_\varphi^{\text{min}}$, where the grains were assumed to be strongly magnetically coupled, the ΔK value should be smaller than that in the case of $\alpha_\varphi^{\text{eff}}=\alpha_\varphi^{\text{int}}$, where the grains were assumed to be magnetically isolated ($\Delta K = K_1$). The fact that a rather good linear fit could be obtained for the temperature-independent α_K suggests that the temperature variation of α_K should be very small. According to this argument, small values of ΔK should be taken in the case that $\alpha_\varphi^{\text{eff}}=\alpha_\varphi^{\text{min}}$ (we take $\Delta K = 0.5K_1$ or $0.1K_1$). If we take the fitted α_K as the value of α_K at room temperature, the value of r_0 can be estimated from Eq. (4). Under the assumption that r_0 is temperature independent, the temperature dependence of α_K can be calculated according to Eq. (4) at various temperatures. However, it is demonstrated from the present calculation that any temperature variation of α_K destroys the linear relationship of H_C/M_s versus $2\alpha_\varphi^{\text{min}}K_1/\mu_0 M_s^2$ as well as of H_C/M_s versus $2\alpha_\varphi^{\text{int}}K_1/\mu_0 M_s^2$ for both $Pr_{17}Fe_{75}B_8$ and $Pr_{17}Fe_{53}B_{30}$ sintered permanent magnets. Following this fact, two points become apparent. First, according to Eq. (4), a very weak temperature dependence of α_K suggests that the values of r_0, the half width of the inhomogeneity range, varies proportionally to δ_B, the domain-wall width, with temperature in Pr-Fe-B magnets. Secondly, the reduction of the second-order anisotropy constant K_1 in the inhomogeneous region in the case that $\alpha_\varphi^{\text{eff}}=\alpha_\varphi^{\text{min}}$ is not so drastic. The nucleation of the reversed domain in this case is localized to the place where the local (micromagnetic) demagnetizing field is the largest, e.g., in close vicinity to holes or sharp corners. Based on this analysis, we obtain $r_0/\delta_B = 0.2152$ ($r_0 = 0.75$ nm at 300 K) in the case that $\alpha_\varphi^{\text{eff}}=\alpha_\varphi^{\text{min}}$ and $r_0/\delta_B = 0.468\,13$ ($r_0 = 1.64$ nm at 300 K) in the case that $\alpha_\varphi^{\text{eff}}=\alpha_\varphi^{\text{int}}$ for $Pr_{17}Fe_{53}B_{30}$; and $r_0/\delta_B = 0.224\,66$ ($r_0 = 0.79$ nm at 300 K) in the case that $\alpha_\varphi^{\text{eff}}=\alpha_\varphi^{\text{min}}$ and $r_0/\delta_B = 0.501\,70$ ($r_0 = 1.76$ nm at 300 K) in the case that $\alpha_\varphi^{\text{eff}}=\alpha_\varphi^{\text{int}}$ for $Pr_{17}Fe_{75}B_8$. It is evident that the value of r_0 obtained when $\alpha_\varphi^{\text{eff}}=\alpha_\varphi^{\text{min}}$ corresponds to the minimum of r_0 and when $\alpha_\varphi^{\text{eff}}=\alpha_\varphi^{\text{int}}$ it corresponds to the maximum. Therefore, the real dimension of the width of the inhomogeneity region ($2r_0$) is between 1.5 and 3.28 nm for $Pr_{17}Fe_{53}B_{30}$ and between 1.58 and 3.52 nm for $Pr_{17}Fe_{75}B_8$ at room temperature.

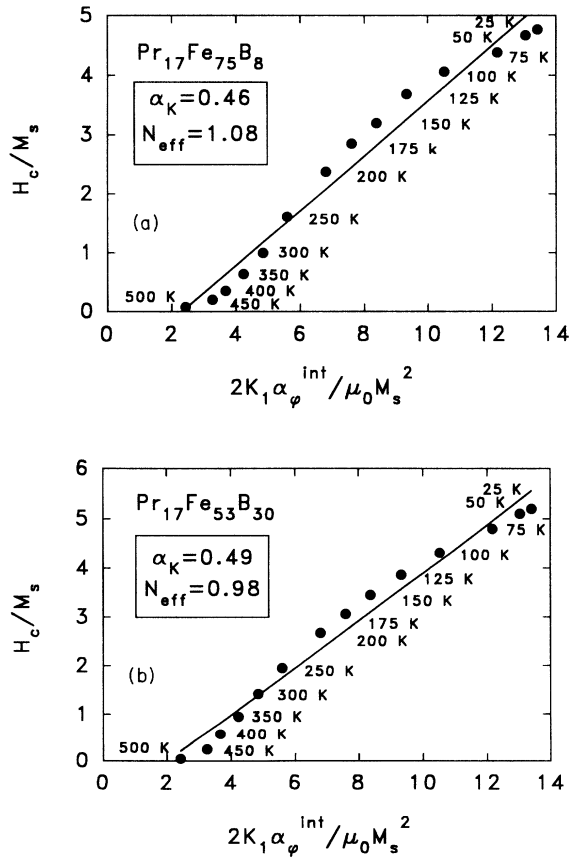

FIG. 12. (a) The plot of H_C/M_s vs $2\alpha_\varphi^{\text{int}}K_1/\mu_0 M_s^2$ for $Pr_{17}Fe_{75}B_8$ for testing the nucleation model under the assumption that grains are magnetically isolated from each other. (b) The plot of H_C/M_s vs $2\alpha_\varphi^{\text{int}}K_1/\mu_0 M_s^2$ for $Pr_{17}Fe_{53}B_{30}$ for testing the nucleation model under the assumption that grains are magnetically isolated from each other.

As it is suggested, $\alpha_\varphi^{\text{min}}$ is the lowest value of $\alpha_\varphi^{\text{eff}}$ and $\alpha_\varphi^{\text{int}}$ the highest value of $\alpha_\varphi^{\text{eff}}$. The real value of $\alpha_\varphi^{\text{eff}}$ should be in between. We therefore assume $\alpha_\varphi^{\text{eff}}=c\alpha_\varphi^{\text{min}}+(1-c)\alpha_\varphi^{\text{int}}$. The value of c can be either determined by the best fitting of the angular dependence of the coercivity or deduced from the experimentally determined N_{eff}. In addition, if we make the plots of H_C/M_s versus $2(c\alpha_\varphi^{\text{min}}+(1-c)\alpha_\varphi^{\text{int}})K_1/\mu_0 M_s^2$, the values of α_K and N_{eff} could be derived from a least-squares-fitting program at various values of c from 0 to 1. It is found from this analysis that the parameters α_K and N_{eff} are not independent from each other. A simple proportional relationship can be deduced for α_K and N_{eff}. In addition, as it was often done,[20,21] the condition that $\alpha_\varphi^{\text{eff}}=\alpha_\varphi^{45^\circ}$ was usually taken. Note that the difference between $\alpha_\varphi^{\text{min}}$ and $\alpha_\varphi^{45^\circ}$ exists only in the low-temperature range (see Fig. 8). Accordingly, a good linear relationship between H_C/M_s and

$2\alpha_\varphi^{45°}K_1/\mu_0 M_s^2$ is found for both $Pr_{17}Fe_{75}B_8$ and $Pr_{17}Fe_{53}B_{30}$ magnets [see Figs. 13(a) and 13(b)]. In the present investigation we have also performed the analysis under the condition of $\alpha_\varphi^{\text{eff}}=\alpha_\varphi^\theta$, where θ varies from 0° to 90°. The fitted values of α_K and N_{eff}, under these conditions, are also plotted in Figs. 14(a) and 14(b) showing a linear relationship. It is evident that these values hold to the proportional relationship between α_K and N_{eff}.

In order to determine the proportionality factor c, a method for direct determination of N_{eff} has been proposed[12] (see Fig. 15). For this experiment, the magnet was assumed to be composed of spherical multidomain grains and the coercivity of the magnet is controlled by the nucleation mechanism. First, the positive magnetic field H_1 (see Fig. 15) is applied to achieve the condition that the domain walls of half of the multidomain grains are eliminated. Then the reversed magnetic field is applied under this condition. In the field range $0<H<H_1$, the magnetization M of the remaining half of the grains

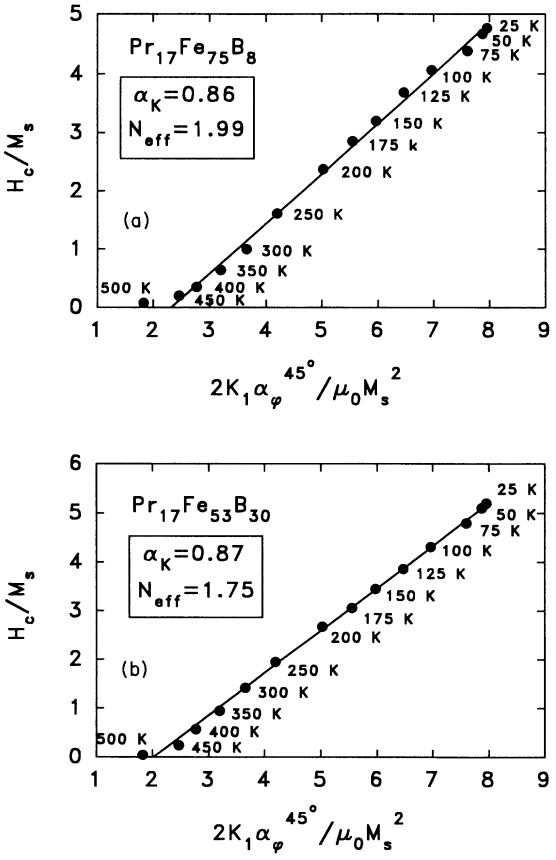

FIG. 13. (a) The plot of H_C/M_s vs $2\alpha_\varphi^{45°}K_1/\mu_0 M_s^2$ for $Pr_{17}Fe_{75}B_8$ for testing the nucleation model under the assumption that the coercivity of magnet is determined by nucleation process occurring in the misaligned grains which make an angle of 45° to the alignment direction. (b) The plot of H_C/M_s vs $2\alpha_\varphi^{45°}K_1/\mu_0 M_s^2$ for $Pr_{17}Fe_{53}B_{30}$ for testing the nucleation model under the assumption that the coercivity of magnet is determined by nucleation process occurring in the misaligned grains, which make an angle of 45° to the alignment direction.

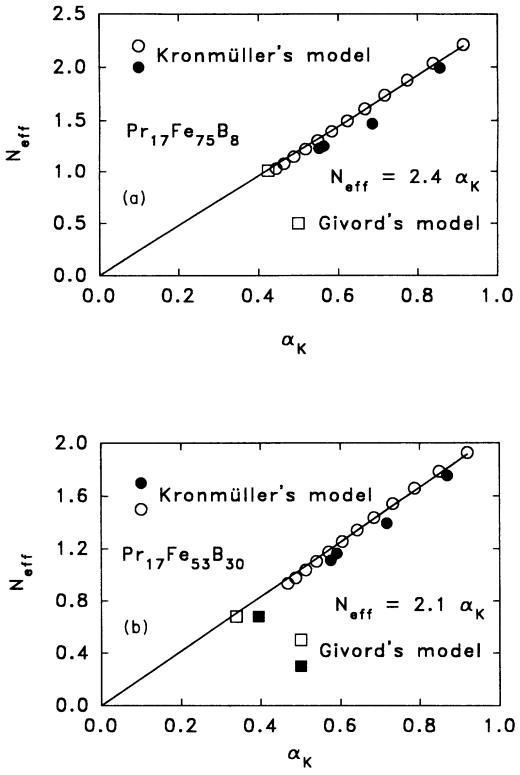

FIG. 14. (a) The fitted linear relationship of N_{eff} and α_K for $Pr_{17}Fe_{75}B_8$. ○ represents the data deduced from the plots of H_C/M_s vs $2[(1-c)\alpha_\varphi^{\min}+c\alpha_\varphi^{\text{int}}]K_1/\mu_0 M_s^2$. ● represents the data deduced from the H_C/M_s vs $2\alpha_\varphi^\theta K_1/\mu_0 M_s^2$, where $\theta=17°$, 20°, 28°, and 45°, respectively (Refs. 4,5,9). □ represents the data deduced from the analysis of phenomenological model (Refs. 10–14). (b) The fitted linear relationship of N_{eff} and α_K for $Pr_{17}Fe_{75}B_8$. ○ represents the data deduced from the plots of H_C/M_s vs $2[(1-c)\alpha_\varphi^{\min}+c\alpha_\varphi^{\text{int}}]K_1/\mu_0 M_s^2$. ● represents the data deduced from the H_C/M_s vs $2\alpha_\varphi^\theta K_1/\mu_0 M_s^2$, where $\theta=17°$, 20°, 28°, and 45°, respectively (Refs. 4,5,9). (□,■) represents the data deduced from the analysis of phenomenological model with different sizes of the reversed domains (Refs. 10–14).

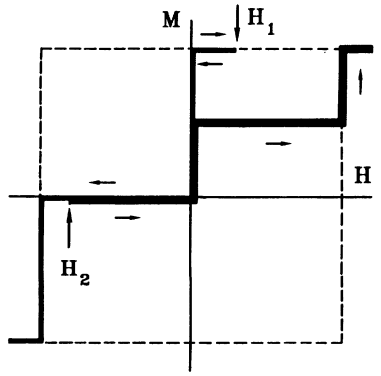

FIG. 15. A proposed ideal experiment for direct determination of the dipolar field between magnetic grains under the coercivity state.

(these still maintain domain walls) will be changed reversibly under the action of the reversed field. On the other hand, the magnetization of the grains with the domain wall being eliminated will remain unchanged. In the field range $H_1<0$, the magnet will remain in the coercivity state ($M=0$) until the coercive field is overcome. Therefore, the dipolar field, the field arising due to the magnetic interaction of the neighboring magnetic grains and needed to nucleate a reversed domain, can be estimated from the negative field H_2, which is required to eliminate the domain walls of half of the grains of the rest half multidomain grains. In this state, only $\frac{1}{4}$ of the total grains is the multidomain grains. In this case the spontaneous magnetization of the neighboring grains is parallel to the applied field. The real demagnetizing field can be obtained from $H_d=H_2+1/3M_s$, where M_s is the spontaneous magnetization of $Pr_2Fe_{14}B$ grains at the measurement temperature and $1/3M_s$ is the demagnetization field of spherical $Pr_2Fe_{14}B$ grains. From the measurement performed at 175 K, Givord *et al.*[12] and Taylor[36] obtained $\mu_0H_2=1.93T$ for $Pr_{17}Fe_{75}B_8$ and $\mu_0H_2=1.59T$ for $Pr_{17}Fe_{53}B_{30}$. From these data, we obtained $\mu_0H_d=2.50T$ for $Pr_{17}Fe_{75}B_8$ and $\mu_0H_d=2.16T$ for $Pr_{17}Fe_{53}B_{30}$ [$\mu_0M_s(175K)=1.70T$]. The N_{eff} value can thereafter be calculated as $N_{\text{eff}}=1.47$ for $Pr_{17}Fe_{75}B_8$ and $N_{\text{eff}}=1.27$ for $Pr_{17}Fe_{53}B_{30}$. Using this data, the proportionality factor c can be determined. We obtained $c=0.48$ for $Pr_{17}Fe_{75}B_8$ and $c=0.41$ for $Pr_{17}Fe_{53}B_{30}$.

How can the physical meaning of these obtained proportionality factors c be understood? It is very unlikely to imagine that $(100c)\%$ of the grains in a magnet are strongly magnetically coupled and the rest ($[100(1-c)]\%$) are magnetically isolated. However, from the microscopically study of permanent magnets[37] it is reasonable to accept that for a grain, statistically, $(100c)\%$ of its surface is strongly magnetically coupled with the neighboring grain surfaces (due to the absence of the grain boundary phases) and the rest of the surface is magnetically isolated (due to the thick grain boundary phases). In addition, it is more reasonable to suggest that in a magnet, statistically, $(100c)\%$ reversed domains are nucleated due to the strongly magnetically coupled neighboring grains (under the minimum nucleation field) and the rest are nucleated individually.

Based on the above discussion, we conclude that in the $Pr_{17}Fe_{75}B_8$ magnet 48% of the grains reverse their magnetization through the reversed domains, which are nucleated due to the strongly magnetically coupled neighboring grains. Thus, at a given temperature nearly half (for $Pr_{17}Fe_{75}B_8$ 48% and $Pr_{17}Fe_{53}B_{30}$ 41%) of the overall grains reverse their magnetization through nucleation of a reversed domain under the condition $\alpha_\varphi^{\text{eff}}=\alpha_\varphi^{\min}$. The field needed to achieve such a state is exactly the coercive field. This gives rise to the reason why a nearly perfect linear relationship is found between H_C/M_s and $2\alpha_\varphi^{\min}K_1/\mu_0M_s^2$ [see Figs. 11(a) and 11(b)] as well as between H_C/M_s and $2\alpha_\varphi^{45°}K_1/\mu_0M_s^2$ [see Figs. 13(a) and 13(b)]. From the above analysis, it is concluded that the coercivity of sintered Pr-Fe-B magnets is controlled by a nucleation mechanism.

VI. GENERAL COMPARISON OF TWO MODELS

A comparison of the two models is made on the following four aspects, namely, (a) theoretical description of the coercive field H_C and the physical meaning of the coefficients α and N_{eff}; (b) the description of the magnetization reversal process; (c) the location of the nucleation of a reversed domain; and (d) conclusions concerning the actual coercivity mechanism for different materials.

A. Theoretical description of the coercive field H_C and the physical meaning of the coefficients α and N_{eff}

For the micromagnetic model, H_C is related to the nucleation field [Eq. (2)]. The physical meaning of the micromagnetic as well as microstructural coefficients is clearly defined in the previous paragraph of the present investigation.

For the phenomenological model, H_C is related to the energy difference of the domain wall at different regions. Let $\gamma=4\sqrt{AK_1}$ and $v_a^{1/3}=\delta=\pi\sqrt{A/K_1}$ be introduced into Eq. (1). Equation (1) then can be rewritten as (the third term is neglected due to its very low value)

$$H_C=\alpha\frac{2}{\pi}\frac{2K_1}{\mu_0M_s}-N_{\text{eff}}M_s \ . \tag{12}$$

As can be clearly seen, Eq. (12) is similar to Eq. (2). However, one should be careful with the assumption $v_a^{1/3}=\delta=\pi\sqrt{A/K_1}$, which is valid only in the temperature range below 500 K (Ref. 36) for a Pr-Fe-B sintered permanent magnet. It is worthwhile to note that the physical meaning changes during the transformation of Eq. (1) into (12). The first term on the right side of Eq. (1) represents the energy barrier, which describes the anisotropy energy at large angles θ (in the domain wall $0°<\theta<\pi$). However, in Eq. (12), the first term on the right represents the nucleation field of a grain, which describes the anisotropy energy at very low angle θ ($\theta\cong0°$) if $K_1>4K_2$.

The physical meaning of coefficient α is not yet well defined. From the definition $\gamma's=\alpha\gamma v^{2/3}$ (γ' is the domain-wall energy at the place, where the reversed domain is nucleated, s is the surface of the reversed domain, γ is the domain-wall energy in the matrix $Pr_2Fe_{14}B$ phase, and v is the activation volume), α must be related in at least two aspects. One originates from the geometry of the reversed domains ($\alpha_1=s/v^{2/3}$), and the other from the inhomogeneity of the domain-wall energy ($\alpha_2=\gamma'/\gamma$). Therefore, α can be expressed by $\alpha=\alpha_1\alpha_2$. The value of α_1 depends strongly on the shape of the nucleated reversed domain. From the observation of the domain structure of Pr-Fe-B as well as Nd-Fe-B magnets, the domains are formed by 180° domain walls and are of platelike shape. Thus, α_1 is calculated for the geometry of Fig. 16, giving

$$\alpha_1=\frac{s}{v^{2/3}}=(9+3\sqrt{5})(\tfrac{2}{9})^{2/3}=5.763$$

under the assumption that $b=3a$. Therefore, it is evident that $2\alpha_2/\pi$ corresponds to $\alpha_\varphi\alpha_K$ of the micromag-

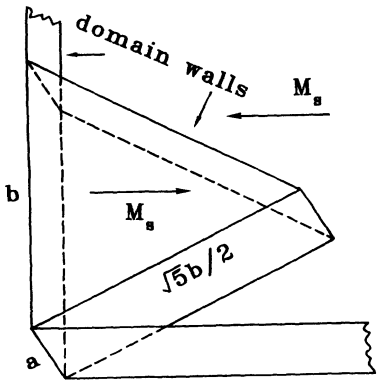

FIG. 16. A proposed geometry of a reversed domain nucleated in a platelike domain of a Pr-Fe-B magnet.

netic model. For a simple comparison, α_φ is taken as 0.661 60, the value of $\alpha_\varphi^{\text{int}}$ at 300 K. α_K is obtained as $\alpha_K=0.424$ for $Pr_{17}Fe_{75}B_8$ and 0.339 for $Pr_{17}Fe_{53}B_{30}$. These values are close to the α_K values obtained in the framework of the micromagnetic model in the case that $\alpha_\varphi^{\text{eff}}=\alpha_\varphi^{\text{int}}$ [Figs. 14(a) and 14(b)].

B. The description of the magnetization reversal process

In the micromagnetic model, the magnetization reversal process is described by a pinning or a nucleation mechanism. In the phenomenological model, the magnetization reversal process is described in a more general way. The magnetization reversal process begins with the formation of a small volume of reversed magnetization and develops with the propagation of this small volume. No specific mechanism is involved.

C. The location of the nucleation of a reversed domain

In the micromagnetic model, the reversed domains are nucleated preferentially in misaligned grains on the grain surface, where the anisotropy is reduced and the local demagnetizing field is the largest. In the phenomenological model, the small volume of reversed domain is nucleated in the region of the grains, where the magnetic properties are different from the bulk properties and the platelike domain is energetically favorable. In the case of multidomain magnets, the nucleation of a reversed domain could be also within the grains at the domain walls.

D. Conclusions concerning the actual coercivity mechanism for different materials

In the micromagnetic model, the analysis has been so far applied to sintered as well as rapidly quenched Nd-Fe-B magnets. The obtained α_K values for various Nd-Fe-B magnets were larger than 0.3. The nucleation mechanism has been proposed to be the leading mechanism controlling the coercivity in these magnets.

In the phenomenological model, the analysis has been applied to various magnets, such as, e.g., $SmCo_5$,[10] Sm_2Co_{17},[13] Nd-Fe-B and ferrite.[10] The obtained N_{eff} values differ from magnet to magnet, however, the α values seem to be independent of the sample and remain close to 1.

VII. SUMMARY AND CONCLUSIONS

In this paper, we have presented a systematic study of the coercivity mechanism of sintered Pr-Fe-B permanent magnets. Two well-established models have been used for this analysis. It is concluded that the nucleation of a reversed domain, occurring preferentially on the grain surface of misaligned grains, is the leading mechanism in determining the coercivity of sintered Pr-Fe-B magnets. From the analysis based on the micromagnetic model it follows that the temperature dependence of the microparameter α_K is very weak. Although the physical meaning is not yet clear, a simple proportional relationship is found between N_{eff} and α_K. Thanks to this analysis, the magnetic coupling between magnetic grains of Pr-Fe-B magnets is estimated. Compared to $Pr_{17}Fe_{75}B_8$, the higher value of the coercive field in $Pr_{17}Fe_{53}B_{30}$ is mainly due to the low value of N_{eff}, suggesting that the $Pr_2Fe_{14}B$ grain surfaces in $Pr_{17}Fe_{53}B_{30}$ are rather smooth and more round. In addition, we have demonstrated that the description of the phenomenological model corresponds roughly to that of the micromagnetic model in the case where magnetic coupling between grains is weak.

ACKNOWLEDGMENTS

The authors thank G. Rieger, J. Bauer, I. Kleinschroth, Dr. W. J. Qiang, Dr. J. Hu, Dr. M. Seeger, and Dr. D. W. Taylor for fruitful discussions and Dr. H. S. Li and Dr. J. M. Cadogan for providing the values of the anisotropy constants, the domain energy, and the domain-wall width. The authors would like to give their particular thanks to Dr. René Pretorius of the National Accelerator Centre of South Africa for critical reading of the manuscript.

[1]K. J. Strnat, in *Ferromagnetic Materials,* edited by E. P. Wohlfarth and K. H. J. Buschow (North-Holland, Amsterdam, 1988), Vol. 4, p. 131.
[2]J. J. Becker, IEEE Trans. Magn. MAG-12, 965 (1976).
[3]H. Kronmüller, Phys. Status Solidi B **144**, 385 (1987).
[4]H. Kronmüller, K.-D. Durst, and G. Martinek, J. Magn. Magn. Mater. **69**, 69 (1987).
[5]H. Kronmüller, K.-D. Durst, and M. Sagawa, J. Magn. Magn. Mater. **74**, 291 (1988).
[6]H. Kronmüller, K.-D. Durst, S. Hock, and G. Martinek, J. Phys. (Paris) Colloq. **49**, C8-623 (1988).
[7]H. Kronmüller, J. Mag. Soc. Jpn. **15**, 6 (1991).

[8]H. Kronmüller, *Science and Technology of Nanostructured Magnetic Materials,* edited by G. C. Hadjipanayis and G. A. Prinz (Plenum, New York, 1991), p. 657.
[9]H. Kronmüller, *Supermagnets, Hard Magnetic Materials,* edited by G. J. Long and F. Grandjean (Kluwer Academic, Dordrecht, 1991), Chap. 19, p. 461.
[10]D. Givord, P. Tenaud, and T. Viadieu, IEEE Trans. Magn. **MAG-24**, 1921 (1988).
[11]D. Givord, P. Tenaud, and T. Viadieu, J. Magn. Magn. Mater. **72**, 247 (1988).
[12]D. Givord, Q. Lu, E. P. Missell, M. F. Rossignol, D. W. Taylor, and V. Villas Boas, J. Magn. Magn. Mater. **104-107**, 1129 (1992).
[13]D. Givord, M. F. Rossignol, D. W. Taylor, and A. E. Ray, J. Magn. Magn. Mater. **104-107**, 1126 (1992).
[14]D. Givord, M. F. Rossignol, and D. W. Taylor, J. Phys. (Paris) IV **2**, 95 (1992).
[15]S. Hirosawa, K. Tokuhara, Y. Matsuura, H. Yamamoto, S. Fujimura, and M. Sagawa, J. Magn. Magn. Mater. **61**, 363 (1986).
[16]Gao Ruwei, Li Hua, Jiang Shouting, Mei Lianmo, and Qiu Meiying, J. Magn. Magn. Mater. **95**, 205 (1991).
[17]W. F. Brown, Jr., Rev. Mod. Phys. **17**, 15 (1945).
[18]J. F. Herbst, Rev. Mod. Phys. **63**, 819 (1991).
[19]G. Martinek and H. Kronmüller, J. Magn. Magn. Mater. **86**, 177 (1990).
[20]G. Martinek and H. Kronmüller, J. Magn. Magn. Mater. **86**, 177 (1990).
[21]G. Martinek, H. Kronmüller, and S. Hirosawa, J. Magn. Magn. Mater. **89**, 369 (1990).
[22]M. Sagawa and S. Hirosawa, J. Mater. Res. **3**, 45 (1988).
[23]M. Sagawa and S. Hirosawa, J. Phys. (Paris) Colloq. **49**, C8-617 (1988).
[24]Jifan Hu, X. C. Kou, and H. Kronmüller, Phys. Status Solidi **138**, L41 (1993).
[25]H. Kronmüller, J. Magn. Magn. Mater. **7**, 341 (1978).
[26]X. C. Kou, T. S. Zhao, R. Grössinger, H. R. Kirchmayr, X. Li, and F. R. de Boer, Phys. Rev. B **46**, 11 204 (1992).
[27]X. C. Kou, T. S. Zhao, R. Grössinger, H. R. Kirchmayr, X. Li, and F. R. de Boer, Phys. Rev. B **47**, 3231 (1993).
[28]J. M. Cadogan, J. P. Gavigan, D. Givord, H. S. Li, J. Phys. F **18**, 779 (1988).
[29]Zhao Tiesong, Jin Hanmin, and Zhu Yong, J. Magn. Magn. Mater. **79**, 159 (1989).
[30]M. Yamada, H. Katao, H. Yamamoto, and Y. Nakagawa, Phys. Rev. B **38**, 620 (1988).
[31]S. Hirosawa, Y. Matsuura, H. Yamamoto, S. Fujimura, M. Sagawa, and H. Yamaauchi, J. Appl. Phys. **59**, 873 (1986).
[32]J. M. Cadogan, D. Givord, H. S. Li, M. F. Rossignol, and D. W. Taylor (unpublished).
[33]H.-R. Hilzinger and H. Kronmüller, Phys. Lett. A **51**, 59 (1975).
[34]H.-R. Hilzinger and H. Kronmüller, Appl. Phys. **12**, 253 (1977).
[35]D. Givord, A. Lienard, R. Perrier de La Bâthie, P. Tenaud, and T. Viadieu, J. Phys. (Paris) Colloq. **46**, C6-313 (1985).
[36]D. W. Taylor, Ph.D. thesis, de l'Institut National Polytechnique de Grenoble, 1992 (unpublished).
[37]G. Schneider, E.-Th. Henig, H. H. Stadelmaier, and G. Petzow (unpublished).
[38]T. Schrefl, H. F. Schmidts, J. Fidler, and H. Kronmüller, J. Appl. Phys. **73**, 6510 (1993).